

## Classification of calcium salts: Correlation of Magnetic Susceptibility With Susceptibility Weighted Imaging (SWI)

A. Fatemi<sup>1</sup>, E. M. Haacke<sup>2,3</sup>, and M. D. Noseworthy<sup>4</sup>

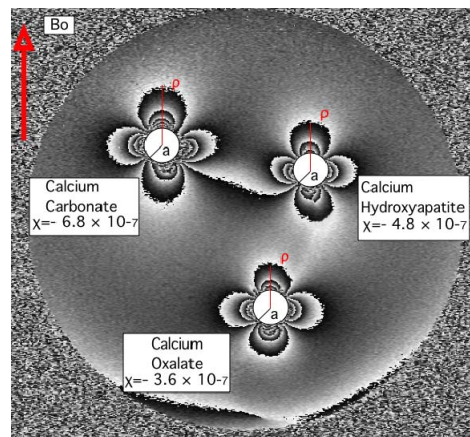
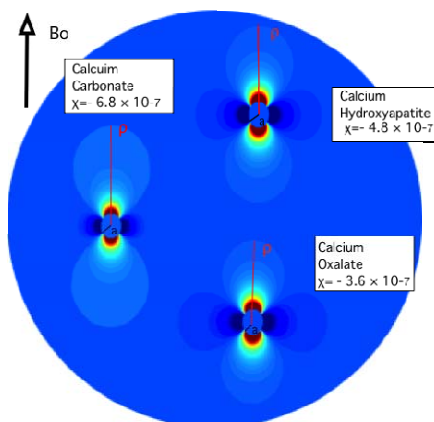
<sup>1</sup>Medical Physics and Applied Radiation Sciences, McMaster University, Hamilton, Ontario, Canada, <sup>2</sup>Radiology, Wayne State University, Detroit, Michigan, United States, <sup>3</sup>The MRI Institute for Biomedical Research, Detroit, Michigan, United States, <sup>4</sup>Electrical and Computer Engineering, School of Biomedical Engineering, McMaster University, Hamilton, Ontario, Canada

### Introduction:

MRI data contains two types of information about local spins, which can be represented as images of either magnitude or phase. In conventional MRI, macroscopic calcification will reduce signal intensity relative to surrounding tissue. We have shown [1] that by using Susceptibility Weighted Imaging (SWI) it is possible to directly detect calcium from corrected phase images. Certain types of calcium salts are extremely important markers of malignancy [2]. We propose that by looking at the local field pattern ( $\Delta\bar{B}$ ) of corrected phase images ( $\varphi = -TE \times \gamma \times \Delta\bar{B}$ ), it is possible to quantify local magnetic susceptibility, which is equivalent to classifying different calcium salts. In this study we are assess the accuracy of our proposed technique by correlating the actual susceptibility values obtained from a susceptibility meter balance with those measured from simulations and phantoms.

### Material and Methods:

The susceptibility of three kinds of calcification was measured [Table 1] by MSB Auto Magnetic Susceptibility Balance [Johnson Matthey USA]. Theoretically, the local field outside an infinite cylinder:



$$\Delta\bar{B}_{external} = \frac{\Delta\chi}{2} \cdot \frac{a^2}{\rho^2} \cdot \sin^2 \theta \cdot \cos 2\phi B_0 + \frac{1}{3} \cdot \chi_e \cdot B_0$$

where  $\chi_i(\chi_e)$  represents the susceptibility inside (outside) the cylinder and  $\Delta\chi = (\chi_i - \chi_e)$ . Predicting magnetic susceptibility from magnetic field is too complicated an inverse problem; therefore, we used a forward, linear approach, working with a known shape/geometry of our source of susceptibility to predict the susceptibility inside of a series of cylinders containing different kinds of calcification. We first simulated the original external field pattern using Matlab for an infinite cylinder (20 pixels diameters) with different susceptibility (volume susceptibility) values [Fig. 1] perpendicular to the external field ( $B_0=7T$ ,  $TE=11ms$ ,  $0.5 \times 0.5 \times 0.5$  isotropic voxel size and  $FOA=10cm$ ). Subsequently, we developed a gel phantom [Fig.2] having three cylindrical calcifications (Calcium Carbonate, Calcium Hydroxyapatite and Calcium Oxalate; Sigma Aldrich) with 20 pixels diameters. Images of this phantom were acquired using a fully flow-compensated 3D SWI sequence on a Bruker 7T MRI ( $TR/TE=50/11ms$ ,  $flip=15^\circ$ ,  $RBW=670$  Hz/pixel, spatial resolution =  $0.5 \times 0.5 \times 0.5$  isotropic voxel size). To reconstruct a perfect susceptibility measurement, using phase images we collected an isotropic high resolution SWI data set, and subsequently high-pass filtered the phase images to remove unwanted background noise and unwrapped phase image.

### Results and Discussion:

[Table 1] shows a volume's susceptibility (multiplied by  $10^7$ ) values, measured using a susceptibility balance, for different kinds of calcification (column 1). Columns two and three report a mean and standard deviation for the estimated volume's susceptibility (multiplied by  $10^7$ ) for three kinds of cylindrical calcifications, from both simulated [Fig.1] and gel phantom data [Fig.2]. The data demonstrate a perfect correlation between susceptibility values measured by a susceptibility balance and those estimate from the simulated and phantom data. Reducing the presence of noise in the phase images is important to improve ones estimate of the true susceptibility value. This can be assessed by setting the phase inside the spherical and cylindrical regions to be constant. Aliasing can also occur due to longer echo times, which can lead to signal loss and aliasing of phase data, and can cause a reduction in the predicted susceptibility inside of each cylinder.

### References:

[1] A. Fatemi-Ardekani, C. Boylan, and M.D. Noseworthy, (2009) *Medical Physics*, 36:5429-5436. [2] A.S. Haka, et al. (2002) *Cancer Res*. 62:5375-5380.

	$\chi_{Actual\ measured}$	$\chi_{Simulation}$ (Mean/SD)	$\chi_{Phantom}$ (Mean/SD)
Calcium Carbonate	$-6.8 \pm 1.7 \times 10^{-5}$	-6.76/0.06	-6.64/0.26
Calcium Hydroxyapatite	$-4.8 \pm 1.2 \times 10^{-5}$	-4.782/0.028	-4.588/0.232
Calcium Oxalate	$-3.6 \pm 9.0 \times 10^{-6}$	-3.576/0.027	-3.385/0.245

**Table 1:** Illustration of susceptibility values (in volume susceptibility  $\times 10^7$ ). First column show an actual measurements of three kind of calcium with susceptibility meter. Second and third columns show means and standard deviations for three types of calcifications susceptibility values from the  $0.5 \times 0.5 \times 0.5$  isotropic voxel data shown in simulation data and phantom data respectively at  $TE=11$  ms.